Andrzej POPENDA

Czestochowa University of Technology
ORCID: 0000-0001-7303-2685

doi:10.15199/48.2025.01.46

Modelling of the BLDC motor taking into account various approximations of the back-EMF waveform

Abstract. *Accurate definition of the back-EMF (electromotive force) waveform, which determines the motor torque, is a very important factor in the design of the drive system. This article proposes formulas for the back-EMF approximation defined on the basis of selected examples of measured waveforms. Next, the influence of various approximations on the behaviour of the motor in steady and unsteady states was examined, using the previously developed mathematical model of the BLDC motor.*

Streszczenie. *Dokładne zdefiniowanie przebiegu siły przeciwelektromotorycznej, która określa moment obrotowy silnika, jest bardzo ważnym czynnikiem przy projektowaniu układu napędowego. W tym artykule zaproponowano formuły aproksymacyjne siły przeciwelektromotorycznej zdefiniowane na podstawie przykładowych przebiegów zmierzonych. Następnie zbadano wpływ różnych aproksymacji na zachowanie silnika w stanie ustalonym i nieustalonym, posiłkując się opracowanym wcześniej modelem matematycznym silnika BLDC. (**Modelowanie silnika BLDC z uwzględnieniem różnych aproksymacji przebiegu siły przeciwelektromotorycznej**)*

Keywords: BLDC motor, modelling and simulation, back-EMF approximation, motor torque.
Słowa kluczowe: silnik BLDC, modelowanie i symulacja, aproksymacja siły przeciwelektromotorycznej, moment silnika.

Introduction

The development of power electronics and the high efficiency of electromechanical energy conversion have made the brushless DC motor (BLDC) more and more often the actuator of industrial drives. The range of applications of BLDC motors includes, above all, a wide range of rotational speeds, sometimes reaching several dozen or even several hundred thousand revolutions per minute. These motors are characterized by high reliability, small dimensions and low rotor inertia. In addition, where there are special requirements regarding operating conditions, such as flammable, corrosive or dusty atmospheres, the use of brushless motors is a must. BLDC motors are widely used in many industries, including the tool industry, automotive, medical, industrial automation, etc.

BLDC motors [1-6] are excited with permanent magnets similarly to PMSMs (permanent magnet synchronous motors) [7,8]. There are two types of permanent magnet motors: motors with a trapezoidal back-EMF (applies mainly to BLDC motors) and motors with a sinusoidal back-EMF (applies mainly to PMSM). This division results from different ways of connecting the coils in the stator winding and different ways of forming the magnetic field distribution in the motor air-gap by appropriate magnetization of permanent magnets or shaping the rotor pole shoes. Motors with sinusoidal back-EMF are characterized by sinusoidal currents and smooth torque, in contrast to the distorted currents and the rippling torque of the motor with a trapezoidal back-EMF, causing additional vibrations and noise.

The waveform of the back-EMF has a significant influence on the torque of the BLDC motor, therefore it is necessary to precisely determine this waveform. Computer simulation tools for the numerical analysis of electric drive systems with BLDC motors commonly use the approximation of the back-EMF to an ideal trapezoidal waveform. But because the shapes of the slot, skew, and magnet of a BLDC motor can be various depending on the design goals, the actual back-EMF waveform may deviate from the ideal trapezoidal waveform. As a consequence, there may be an error between the actual value and the simulation result when using ideal trapezoids to approximate the back-EMF. This article proposes formulas for the back-EMF approximation defined on the basis of selected examples of measured waveforms. Next, the influence of various approximations on the behaviour of the motor in steady and unsteady states was examined, using the previously developed mathematical model of the BLDC motor.

Approximation of the back-EMF of a BLDC motor

As mentioned in the introduction, computer simulation tools for numerical analysis of electric drive systems with BLDC motors usually use the approximation of the back-EMF to an ideal trapezoidal waveform. The mathematical formula to describe this approximation for a three-phase BLDC motor was proposed in [1]. For this purpose, the back-EMFs induced in the motor phase windings were expressed in a matrix form as the product of the number of pole pairs N_p, the flux linkage Ψ_P excited by the rotor's permanent magnets, the angular velocity of the rotor ω_m and the shape functions given as a column vector $\mathbf{f}$:

$$\mathbf{e} = N_p \Psi_P \omega_m \mathbf{f} \tag{1}$$

where $\mathbf{e} = [e_a \quad e_b \quad e_c]^{\mathrm{T}}$ is the column vector of the back electromotive forces induced in the motor phase windings and $\mathbf{f} = [f_a(\theta_e) \quad f_b(\theta_e) \quad f_c(\theta_e)]^{\mathrm{T}}$ is the column vector of the shape functions. In order to approximate the shape functions, the following dependencies were adopted [1]:

$$\begin{aligned} f_a(\theta_e) &= k_f \sin(\theta_e) \quad \cap \quad |f_a(\theta_e)| \le 1 \\ f_b(\theta_e) &= k_f \sin\left(\theta_e - \tfrac{2\pi}{3}\right) \quad \cap \quad |f_b(\theta_e)| \le 1 \\ f_c(\theta_e) &= k_f \sin\left(\theta_e - \tfrac{4\pi}{3}\right) \quad \cap \quad |f_c(\theta_e)| \le 1 \end{aligned} \tag{2}$$

where $k_f = 2$ was taken into account for the trapezoidal back-EMF approximation with a wide trapeze base (120 electrical degrees), $\theta_e = N_p \theta_m$, $\theta_e \in [0°; 360°)$, θ_m is the angle of rotor's rotation.

Meanwhile, the literature sources often report imprecision of such an approximation in relation to the actual waveform of the back-EMF. In the paper [2], attention was paid to the influence of the shape of the slot, skew and magnet of the BLDC motor, which may be different depending on the design goals, therefore the actual waveform of the back-EMF may differ from the ideal trapezoidal waveform. Paper [3] presents the results of the back-EMF measurement of a high-speed BLDC motor with claw poles based rotor. The

results of this measurement in the form of points are shown in Figure 1. The same figure also shows the proposed back-EMF approximation (solid line) according to the following shape functions:

$$f_a(\theta_e) = \sin\left(\frac{\pi}{2}\sin\theta_e\right)$$

$$f_b(\theta_e) = \sin\left(\frac{\pi}{2}\sin\left(\theta_e - \frac{2\pi}{3}\right)\right) \quad (3)$$

$$f_c(\theta_e) = \sin\left(\frac{\pi}{2}\sin\left(\theta_e - \frac{4\pi}{3}\right)\right)$$

Comparison of the proposed approximation with the measurement points shows a good representation of the actual values. The paper [4] presents the measured back-EMF waveform of a low-power BLDC motor. This waveform (dashed line) together with the approximation proposed in this article (solid line) is shown in Figure 2. The shape functions for the respective motor phases, corresponding to the aforementioned approximation, are given as follows:

$$f_a(\theta_e) = \sin\left(\frac{\pi}{2}\sin^p\left(\frac{\pi}{2}\sin\theta_e\right)\right)$$

$$f_b(\theta_e) = \sin\left(\frac{\pi}{2}\sin^p\left(\frac{\pi}{2}\sin\left(\theta_e - \frac{2\pi}{3}\right)\right)\right) \quad (4)$$

$$f_c(\theta_e) = \sin\left(\frac{\pi}{2}\sin^p\left(\frac{\pi}{2}\sin\left(\theta_e - \frac{4\pi}{3}\right)\right)\right)$$

where $p = m/n$, m and n are odd numbers; the current approximation assumes $m = 17$ and $n = 5$. Also in this case, the approximation correctly estimates the actual back-EMF waveform. Figure 3 shows the waveforms of the back-EMF for different p values, approximated according to the first shape function from the set (4), thus indicating the universality of the proposed formula in terms of various approximations.

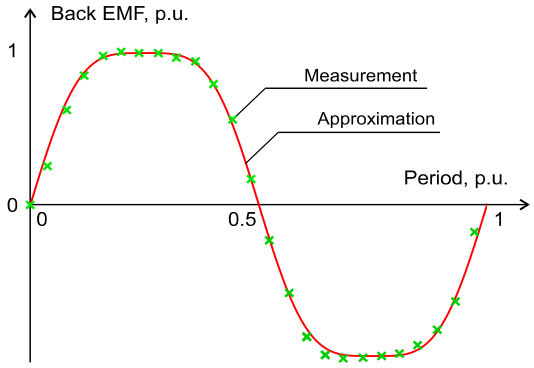

Fig. 1. Back-EMF waveform, measured and approximated according to the first shape function from the set (3)

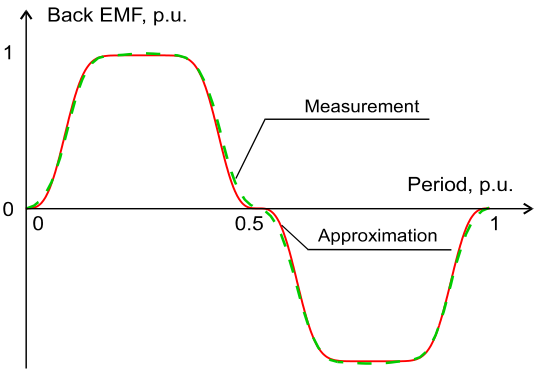

Fig. 2. Back-EMF waveform, measured and approximated according to the first shape function from the set (4)

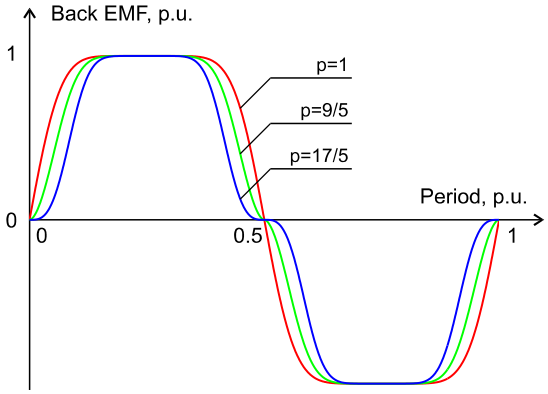

Fig. 3. Back-EMF waveforms for different p values, approximated according to the first shape function from the set (4)

Mathematical model of the BLDC motor

In paper [1], a mathematical model of a three-phase BLDC motor was proposed and the results of computer simulation and experimental verification were presented. The comparison of these results showed a high adequacy of the proposed model. This model is based on the equivalent circuit of an inverter-fed BLDC motor. In paper [5] the abovementioned model was presented in matrix form:

$$\mathbf{u} = R\mathbf{i} + \dot{\boldsymbol{\psi}} + \mathbf{e} \quad (5)$$

where $\mathbf{u} = [u_a \;\; u_b \;\; u_c]^{\mathrm{T}}$, $\mathbf{i} = [i_a \;\; i_b \;\; i_c]^{\mathrm{T}}$ and $\boldsymbol{\psi} = [\psi_a \;\; \psi_b \;\; \psi_c]^{\mathrm{T}}$ are the column vectors of the terminal voltages, phase currents and phase flux linkages of the motor, respectively,

$$\mathbf{i} = (L - M)^{-1}(\boldsymbol{\psi} + M\mathbf{i}_0) \quad (6)$$

$$i_0 = (L + 2M)^{-1}(\psi_a + \psi_b + \psi_c) \quad (7)$$

where $\mathbf{i}_0 = [i_0 \;\; i_0 \;\; i_0]^{\mathrm{T}}$ is the vector of the phase currents' sums, i.e. $i_0 = i_a + i_b + i_c$, L is the phase self-inductance of the motor winding: $L = L_\sigma + L_{ar}$, L_σ is the leakage inductance, L_{ar} is the armature reaction inductance, M is the mutual inductance between the motor phase windings: $M = -L_{ar}/3$ or $-L_{ar}/2$ depending on the design of the motor winding, then $L - M = L_\sigma + 4L_{ar}/3$ or $L_\sigma + 3L_{ar}/2$, respectively.

The equation of motion of the rotor and the rotating masses attached to it is as follows:

$$\frac{d^2}{dt^2}\theta_m = \frac{d}{dt}\omega_m = J^{-1}(\tau_e - \tau_L) \quad (8)$$

where J is the moment of rotor's inertia, τ_L is the load torque and τ_e is the motor torque:

$$\tau_e = N_p \Psi_P \mathbf{f}^{\mathrm{T}}\mathbf{i} \quad (9)$$

The conventional approach to BLDC motor control is based on the logic states of Hall sensors subjected to the magnetic field of the rotor with permanent magnets. Hall sensors mounted in the stator together with the rotor's permanent magnets form a magnetic encoder which, in the case of a three-phase motor, allows the angular position of the rotor to be measured with an accuracy of 60 electrical degrees. The three-phase BLDC motor control strategy, based on the logic states generated by the magnetic encoder, is presented in [1]. For the selected range of the rotor's angular position: $30° < \theta_e \leq 90°$, the following dependencies can be written:

$$u_0 = R_0 i_0, \qquad u_a = \tfrac{1}{2} u_d - u_0, \qquad u_b = -\tfrac{1}{2} u_d - u_0$$

(10)

$$u_{c0} = \tfrac{1}{2} R_{off} i_c \;\cap\; -\tfrac{1}{2} u_d \le u_{c0} \le +\tfrac{1}{2} u_d, \qquad u_c = -u_{c0} - u_0$$

where u_d is the DC source voltage, R_0 is the neutral conductor resistance; $R_0 = \infty$ in the case of a motor energized without neutral conductor. Instead of $R_0 = \infty$, for numerical calculations, a sufficiently large value of the resistance R_0 can be adopted, i.e. several orders of magnitude greater than the rated impedance defined on the basis of the rated phase parameters of the motor, i.e. $R_0 >> U_{n(ph)} / I_{n(ph)}$. The dependencies are analogous to (10) for the successive ranges of the rotor's angular position. Controlling the BLDC motor with the use of logic states generated by the magnetic encoder enables the motor's phase windings to be energized with voltage of a trapezoidal waveform.

Computer simulation results

The following rated parameters of the BLDC motor were taken into account in the simulation tests: 4 kW, 400 V, 1500 rpm, 11.5 A, 0.025 kgm^2, R_s = 0.5 Ohm, L_{ar} = 7.4 mH, L_σ = 1.6 mH, $N_p \omega_n \Psi_P$ = 170 V. In the simulation tests performed, the motor was connected to a set of rotating masses, which together with the steel drive shaft formed a dual-mass system [9,10]. The motor was loaded with the rated braking torque via the abovementioned working mechanism. Figures 4 to 9 show the characteristic quantities of the BLDC motor as a function of time when the motor is controlled without closed loops for current and angular velocity. Motor starting is performed by changing the supply voltage from zero to a fixed level according to the time ramp function. Figures 4, 5 and 6 show the time responses of the BLDC motor during start-up and during operation under rated load, while Figures 7, 8 and 9 show the waveforms for the BLDC motor under load in the selected time interval.

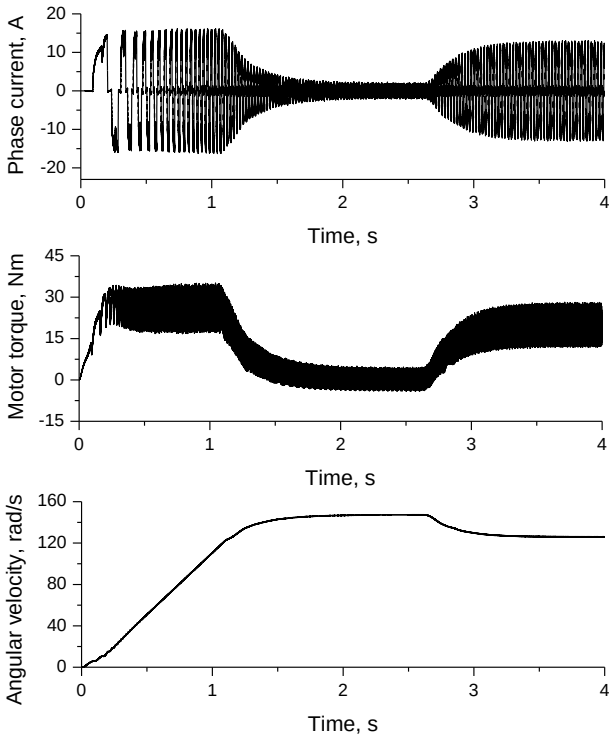

Fig. 4. Time responses of the BLDC motor: phase current, motor torque and angular velocity for the trapezoidal approximation of the back-EMFs according to the shape functions (2)

Figures 4 and 7 show the characteristic quantities of the BLDC motor for the trapezoidal approximation of the back-EMFs according to the shape functions (2), whereas Figures 5 and 8 and Figures 6 and 9 show the characteristic quantities for the approximation of the back-EMFs according to the shape functions (3) and (4), respectively.

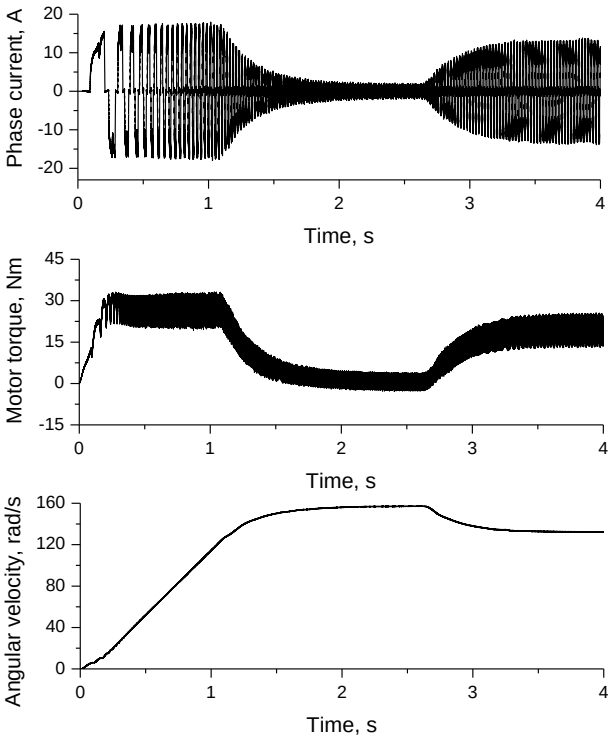

Fig. 5. Time responses of the BLDC motor: phase current, motor torque and angular velocity for the approximation of the back-EMFs according to the shape functions (3)

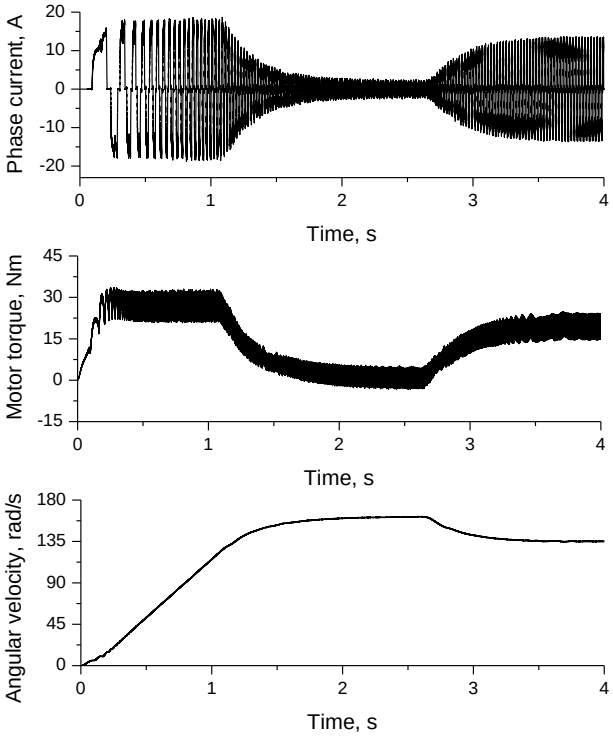

Fig. 6. Time responses of the BLDC motor: phase current, motor torque and angular velocity for the approximation of the back-EMFs according to the shape functions (4)

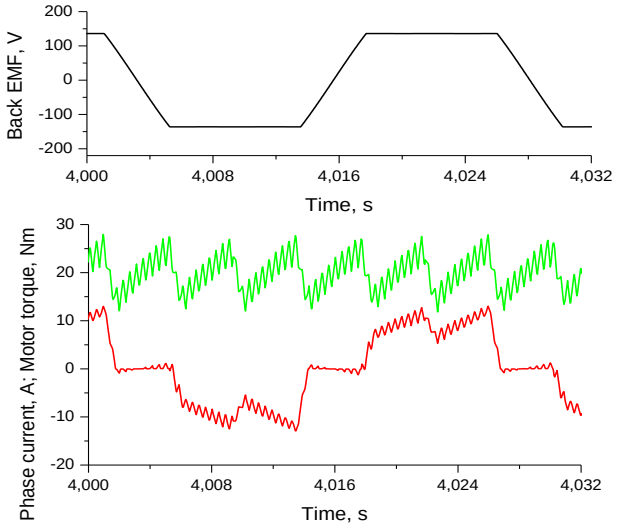

Fig. 7. Back-EMF, torque and phase current waveforms of BLDC motor for the trapezoidal approximation of the back-EMFs according to the shape functions (2)

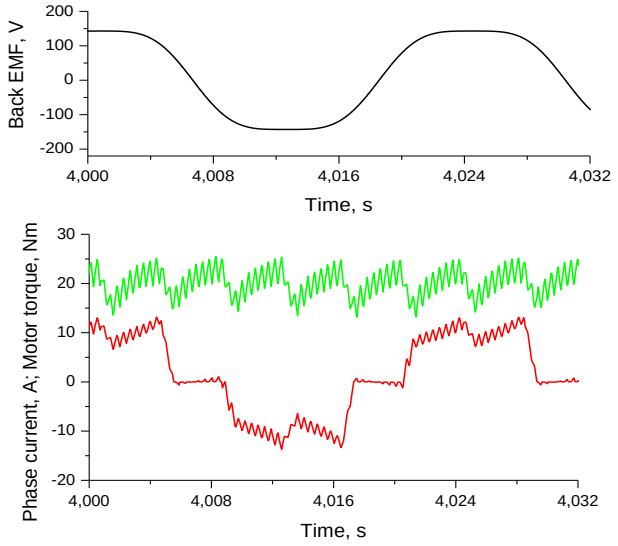

Fig. 8. Back-EMF, torque and phase current waveforms of BLDC motor for the approximation of the back-EMFs according to the shape functions (3)

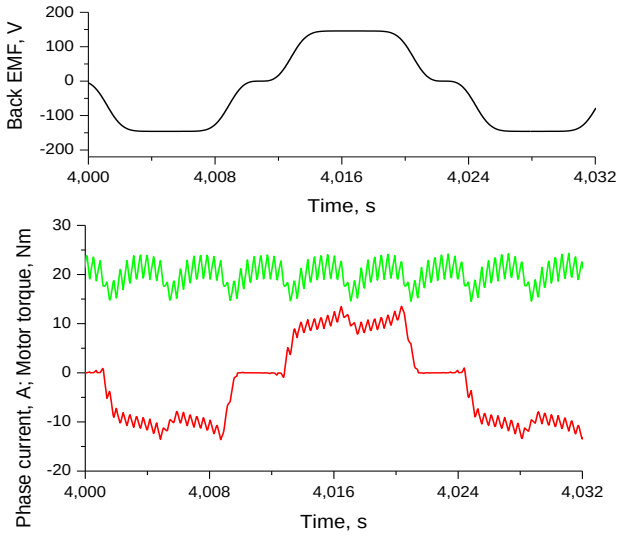

Fig. 9. Back-EMF, torque and phase current waveforms of BLDC motor for the approximation of the back-EMFs according to the shape functions (4)

Conclusions

In this paper, formulas for approximation of the back-EMF induced in the phase windings of a BLDC motor were proposed. Above the formulas have been defined on the basis of sample measured waveforms. Accurate definition of the back-EMF waveform, which determines the motor torque, is a very important factor in the design of the drive system. In the further part of the article, the results of simulation tests are presented, taking into account the proposed approximations of the back-EMF. The following conclusions can be formulated on the basis of the conducted research.

The motor torque ripple with the largest amplitude occurs when the trapezoidal back-EMF approximation is adopted (see Figures 4 and 7), while in the other two cases the amplitude of the torque ripple is comparable. Less torque ripple does not mean less current amplitude. Then the situation is different, i.e. the phase current with the smallest amplitude corresponds to the trapezoidal approximation of the back-EMF, especially during starting the motor, however, this approximation also corresponds to the lowest level of steady-state angular velocity after the end of starting the motor (compare figures 4, 5 and 6). The higher the level of steady-state angular velocity after the end of starting the motor, the greater the current drawn by the motor when starting with the same time ramp of the supply voltage. This is also related to the RMS value of the back-EMF, which is the largest in the case of the trapezoidal approximation. On the other hand, various back-EMF approximations do not significantly affect the dynamics of the drive unit based on the BLDC motor.

Author: *Andrzej Popenda, PhD, D.Sc., Associate Prof., Czestochowa University of Technology, Faculty of Electrical Engineering, 17 Armii Krajowej av, 42-200 Częstochowa, E-mail: andrzej.popenda@pcz.pl*

REFERENCES

[1] Popenda A., Modelling of BLDC motor energized by different converter systems, *Przegląd Elektrotechniczny*, 94 (2018), no. 1, 81-84

[2] Jeon Y.S., Mok H.S., Choe G.H., Kim D.K., Ryu J.S., A New Simulation Model of BLDC Motor With Real Back EMF Waveform, *7th Workshop on Computers in Power Electronics (COMPEL 2000)*, Blacksburg, VA, USA, 16-18 July 2000, 217-220

[3] Huang Y., Zhu J., Guo Y., Hu Q., Development of a High-Speed Claw Pole Motor with Soft Magnetic Composite Core, *IEEE International Electric Machines & Drives Conference (IEMDC'07)*, IEEE International, Antalya, Turkey, 3-5 May 2007, Vol. 2, 1564-1568

[4] Goryca Z., Bezszczotkowe silniki prądu stałego – konstrukcje i sterowanie, *Automatyka – Elektryka – Zakłócenia*, (2013), nr 3, 56-63

[5] Popenda A., Nowak M., Modelling of an optimized BLDC motor energized by a sinusoidal voltage source, *Przegląd Elektrotechniczny*, 99 (2023), no. 2, 250-254

[6] Shchur I., Lis M., Biletskyi Y., Passivity-Based Control of Water Pumping System Using BLDC Motor Drive Fed by Solar PV Array with Battery Storage System, *Energies*, 14 (2021), no. 8184, 1-25

[7] Szafraniec A., Mathematical model of a drive system with synchronous motors and vertical pumps, *E3S Web of Conferences (PE 2018)*, 84 (2019), no. 02015, 1-9

[8] Olesiak K., Application of a Fuzzy Logic Controller for a Permanent Magnet Synchronous Machine Drive, *Przegląd Elektrotechniczny*, 92 (2016), no. 12, 113-116

[9] Popenda A., Szafraniec A., Chaban A., Dynamics of Electromechanical Systems Containing Long Elastic Couplings and Safety of Their Operation, *Energies*, 14 (2021), no. 7882, 1-18

[10] Kabziński J., Mosiołek P., Observer-Based, Robust Position Tracking in Two-Mass Drive System, *Energies*, 15 (2022), no. 9093, 1-28